

1 **Erosion of organic carbon in the Arctic as a geological carbon dioxide sink**

2 Robert G. Hilton<sup>1\*</sup>, Valier Galy<sup>2</sup>, Jérôme Gaillardet<sup>3</sup>, Mathieu Dellinger<sup>3</sup>, Charlotte Bryant<sup>4</sup>,  
3 Matt O'Regan<sup>5</sup>, Darren R. Gröcke<sup>6</sup>, Helen Coxall<sup>5</sup>, Julien Bouchez<sup>3</sup>, & Damien Calmels<sup>7</sup>

4 <sup>1</sup>Department of Geography, Durham University, South Road, Durham, DH1 3LE, UK

5 <sup>2</sup>Department of Marine Chemistry and Geochemistry, Woods Hole Oceanographic Institution, 266  
6 Woods Hole Rd., Woods Hole, MA 02543-1050, USA

7 <sup>3</sup>Institut de Physique du Globe de Paris, Sorbonne Paris Cité, Univ Paris Diderot, UMR 7154 CNRS,  
8 F-75005 Paris, France

9 <sup>4</sup>NERC Radiocarbon Facility, East Kilbride, Scotland, G75 0QF, UK

10 <sup>5</sup>Department of Geological Sciences, Stockholm University, Sweden

11 <sup>6</sup>Department of Earth Sciences, Durham University, South Road, Durham, DH1 3LE, UK

12 <sup>7</sup>Université Paris-Sud, Laboratoire GEOPS, UMR 8148 - CNRS, Orsay, F-91405, France

13

14 \*To whom correspondence should be addressed. Email: r.g.hilton@durham.ac.uk. Phone: 0044 0191  
15 33 41970

16 **Soils of the northern high latitudes store carbon over millennial timescales ( $10^3$  yrs) and**  
17 **contain approximately double the carbon stock of the atmosphere<sup>1-3</sup>. Warming and**  
18 **associated permafrost thaw can expose soil organic carbon and result in mineralisation**  
19 **and carbon dioxide (CO<sub>2</sub>) release<sup>4-6</sup>. However, some of this soil organic carbon may be**  
20 **eroded and transferred to rivers<sup>7-9</sup>. If it escapes degradation during river transport and**  
21 **is buried in marine sediments, then it can contribute to a longer-term ( $>10^4$  yrs),**  
22 **geological CO<sub>2</sub> sink<sup>8-10</sup>. Despite this recognition, the erosional flux and fate of**  
23 **particulate organic carbon (POC) in large rivers at high latitudes remains poorly**  
24 **constrained. Here, we quantify POC source in the Mackenzie River, the main sediment**  
25 **supplier to the Arctic Ocean<sup>11,12</sup> and assess its flux and fate. We combine measurements**

26 **of radiocarbon, stable carbon isotopes and element ratios to correct for rock-derived**  
27 **POC<sup>10,13,14</sup>. Our samples reveal that the eroded biospheric POC has resided in the basin**  
28 **for millennia, with a mean radiocarbon age of 5800±800 yr, much older than large**  
29 **tropical rivers<sup>13,14</sup>. Based on the measured biospheric POC content and variability in**  
30 **annual sediment yield<sup>15</sup>, we calculate a biospheric POC flux of 2.2<sup>+1.3</sup><sub>-0.9</sub> TgC yr<sup>-1</sup> from**  
31 **the Mackenzie River, three times the CO<sub>2</sub> drawdown by silicate weathering<sup>16</sup>. Offshore**  
32 **we find evidence for efficient terrestrial organic carbon burial over the Holocene,**  
33 **suggesting that erosion of organic carbon-rich, high latitude soils may result in a**  
34 **significant geological CO<sub>2</sub> sink.**

35 Photosynthesis and the production of organic carbon by the terrestrial biosphere  
36 (OC<sub>biosphere</sub>) is a major pathway of atmospheric carbon dioxide (CO<sub>2</sub>) drawdown. Over  
37 millennial timescales (10<sup>3</sup> yrs), some OC<sub>biosphere</sub> escapes oxidation and contributes to a  
38 transient CO<sub>2</sub> sink in soil<sup>2,3,17</sup>. Longer-term CO<sub>2</sub> drawdown (>10<sup>4</sup> yrs) can be achieved if  
39 OC<sub>biosphere</sub> is eroded, transferred by rivers and buried in sedimentary basins<sup>9,10,18,19</sup>. Burial of  
40 OC<sub>biosphere</sub> represents a major geological CO<sub>2</sub> sink (and O<sub>2</sub> source) alongside the chemical  
41 weathering of silicate minerals by carbonic acid, coupled to carbonate precipitation<sup>16,19</sup>.  
42 These fluxes negate CO<sub>2</sub> emissions from the solid Earth<sup>20</sup> and from oxidation of rock-derived  
43 OC<sup>21</sup>, contributing to the long-term regulation of global climate<sup>19,20</sup>. Physical erosion is  
44 thought to play a significant role in this OC<sub>biosphere</sub> transfer because it controls the rate of  
45 biospheric particulate organic carbon (POC<sub>biosphere</sub>) export by rivers<sup>22</sup> and influences sediment  
46 accumulation and the efficiency of OC burial<sup>10,18,23</sup>.

47 In the northern high latitudes, large amounts of OC<sub>biosphere</sub> are stored in soil<sup>1,2</sup>. The  
48 upper three meters of soil in the region of northern circumpolar permafrost are estimated to  
49 contain 1035±150 PgC, approximately double the carbon dioxide (CO<sub>2</sub>) content of the pre-  
50 industrial atmosphere<sup>17</sup>. Many of these soils accumulated during the retreat of large

51 continental ice sheets following the Last Glacial Maximum, with a peak expansion between  
52 12,000 and 8,000 cal. yr BP<sup>24</sup> and the OC<sub>biosphere</sub> can be thousands of years old<sup>8</sup>. This vast  
53 carbon reservoir is located in a region sensitive to environmental change over glacial-  
54 interglacial timescales<sup>24</sup> and to warming over the coming century<sup>3</sup>. Much focus has been  
55 placed on its potential to become a CO<sub>2</sub> source<sup>3-6,8</sup>. However, geological CO<sub>2</sub> drawdown by  
56 POC<sub>biosphere</sub> erosion at high latitudes has remained poorly constrained<sup>9</sup>.

57 Here we sample POC carried by the major rivers in the Mackenzie Basin and  
58 investigate its fate using an offshore sediment core extending over the Holocene (Extended  
59 Data Fig. 1). The Mackenzie River is the largest source of sediment to the Arctic Ocean<sup>11,12,15</sup>  
60 and erosion of mountainous topography in the basin results in a high sediment discharge,  
61 similar to the combined total of 16 Eurasian rivers draining to the Arctic<sup>11,15</sup>. We collected  
62 river depth profiles to characterise POC across the range of grain sizes carried by large  
63 rivers<sup>13,14,25</sup> at the main conduit for sediment export to the Arctic Ocean in the Mackenzie  
64 Delta, at key points on the Mackenzie River and from its major tributaries (Extended Data  
65 Fig. 1). To investigate temporal variability of POC composition, river depth profiles were  
66 collected shortly after ice-break up at high/rising stage (June 2011) and during falling stage  
67 (September 2010), while river surface and bank samples were collected in June 2009. To  
68 correct for rock-derived, ‘petrogenic’ POC (POC<sub>petro</sub>), likely to be important in the  
69 Mackenzie Basin<sup>7,25</sup>, we combine measurements of radiocarbon (<sup>14</sup>C, reported as the ‘fraction  
70 modern’ F<sub>mod</sub>), total OC content ([OC<sub>total</sub>], %), stable isotopes of OC ( $\delta^{13}\text{C}_{\text{org}}$ ), nitrogen to OC  
71 ratio (N/OC<sub>total</sub>) and aluminium to OC ratio (Al/OC<sub>total</sub>), which allow us to assess the age and  
72 concentration of POC<sub>biosphere</sub> (Methods)<sup>7,10,13,14,22</sup>. Published surface samples from the  
73 Mackenzie River<sup>4,7</sup> (n=5) have <sup>14</sup>C-ages between 6,010 yr and 10,000 yr but the <sup>14</sup>C-depletion  
74 caused by POC<sub>petro</sub> versus aged POC<sub>biosphere</sub> has not been assessed. We also examine the

75 hydrodynamic behaviour of POC, using the aluminium to silicon ratio (Al/Si) ratio as a proxy  
76 of sediment grain size<sup>25</sup>.

77 We find that river POC is <sup>14</sup>C-depleted throughout the Mackenzie Basin (Extended  
78 Data Table 1).  $F_{mod}$  values range between 0.28 (<sup>14</sup>C age = 10,106±42 yr) and 0.63 (<sup>14</sup>C age =  
79 3675±36 yr) in the suspended load (n=27) and  $F_{mod}$  = 0.12 (<sup>14</sup>C age = 17,002±84 yr) to 0.16  
80 (<sup>14</sup>C age = 14,601±64 yr) in the river bed materials (n=4). To investigate the cause of this  
81 <sup>14</sup>C-depletion, we examine the N/OC<sub>total</sub> ratio. Degradation of organic matter in soils can  
82 increase the relative N abundance<sup>6,26</sup>, differentiating degraded POC<sub>biosphere</sub> (high N/OC<sub>total</sub>)  
83 from young, fresh POC<sub>biosphere</sub> (low N/OC<sub>total</sub>). Suspended load samples display a negative  
84 relationship between N/OC<sub>total</sub> and  $F_{mod}$  (Fig. 1), similar to measurements from a peat core in  
85 the Mackenzie Basin<sup>26</sup> away from permafrost. There, N/OC<sub>total</sub> ratios increased with <sup>14</sup>C age  
86 (1,250 yr to 10,200 yr) and soil depth (0m to 3m). In contrast, river bed materials have lower  
87  $F_{mod}$  values and a relatively restricted range of N/OC<sub>total</sub> values and are distinct from  
88 suspended load (Fig. 1). A dominance of POC<sub>petro</sub> in bed materials<sup>10,14</sup> with a N/OC<sub>total</sub> ratio  
89 of ~0.07 can explain their composition.

90 Together, the  $F_{mod}$  and N/OC<sub>total</sub> values suggest that POC in the Mackenzie River is a  
91 mixture of POC<sub>petro</sub> and POC<sub>biosphere</sub>, itself varying in <sup>14</sup>C age from ‘modern’ to ~8000 yrs  
92 (Fig. 1). The  $\delta^{13}\text{C}_{org}$  values and Al/OC<sub>total</sub> ratios support this inference (Extended Data Fig. 2).  
93 Using an end member mixing analysis<sup>10,13</sup> we quantify POC<sub>petro</sub> content of sediments  
94 (Methods) and find that suspended load at the Mackenzie River Delta is dominated by  
95 POC<sub>biosphere</sub> (~70-90% of the total POC). Having corrected for POC<sub>petro</sub>, we investigate the  
96 source of POC<sub>biosphere</sub> by estimating its average <sup>14</sup>C age. This varies from 3030±150 yr to  
97 7900±400 yr (Extended Data Fig. 3) with an average <sup>14</sup>C age of POC<sub>biosphere</sub> = 5800±800 yr  
98 (±2SE) in suspended sediments of the Mackenzie River Delta. These values are older than  
99 estimates of POC<sub>biosphere</sub> age from the Amazon River (1120-2750 yr)<sup>14</sup> and Ganges River

100 (1600-2960 yr)<sup>13</sup>. The ages reflect mixing of young, fresh POC<sub>biosphere</sub> present in each of these  
101 large river basins, with an older POC<sub>biosphere</sub> in the Mackenzie Basin (Fig. 1), likely to be  
102 peats which expanded between 9,000 yr and 8,000 yr (<sup>14</sup>C-age)<sup>24</sup>. POC<sub>biosphere</sub> can be eroded  
103 by slumping and landsliding on river banks, across deep soil profiles<sup>4,7</sup>. Sections of the  
104 landscape which have discontinuous permafrost and those undergoing permafrost  
105 degradation<sup>27</sup> may be important sources of aged POC<sub>biosphere</sub>, in addition to river banks which  
106 are undercut during peak water discharge following ice-break up<sup>15</sup>. Our samples suggest that  
107 erosion and fluvial transfer of millennial-aged POC<sub>biosphere</sub> is extensive in the Mackenzie  
108 Basin.

109 Once in the river, POC<sub>biosphere</sub> is sorted with river depth, revealed by the Al/Si ratio  
110 (Fig. 2b) a proxy for grain size<sup>25</sup>. In bed materials with low Al/Si, POC<sub>petro</sub> dominates (Fig. 1)  
111 and leads to low F<sub>mod</sub> values (Fig. 2c). Just above the river bed, during the two sampling  
112 campaigns coarse suspended sediments (low Al/Si) hosted the youngest, least degraded  
113 POC<sub>biosphere</sub> (low N/C) leading to a significant contrast in <sup>14</sup>C age from the bed materials.  
114 Towards the river surface, older, more degraded POC<sub>biosphere</sub> appears to dominate, and is  
115 transported with fine sediment and clays (high Al/Si)<sup>25</sup>. The significant contribution of  
116 degraded, very old POC<sub>biosphere</sub> (>5000 yrs) contrasts with large tropical rivers where organic  
117 matter turnover in terrestrial ecosystems is more rapid (Fig. 2c)<sup>13,14</sup>.

118 To assess how erosion in the Mackenzie River may lead to long-term CO<sub>2</sub> drawdown,  
119 we estimate POC<sub>biosphere</sub> discharge. River depth profiles collected at high and falling stage  
120 suggest that the [OC<sub>total</sub>] of the suspended sediment load did not vary systematically with  
121 sediment grain size (Extended Data Fig. 4). Future work should seek to assess temporal  
122 variability in POC content and composition. Our samples suggest that changes in grain size  
123 with water discharge (Fig. 2b) could be important in setting the variability of POC<sub>biosphere</sub> age  
124 carried by the river (Fig. 2c). The [OC<sub>total</sub>] values at the Delta were 1.6±0.5% (n=8, ±1σ),

which were similar to the mean measured in the Mackenzie Delta in June-July 1987 of  $1.4 \pm 0.2$  ( $n=10$ )<sup>12</sup>. While our sample set is modest in size, it helps us to better constrain the range of POC contents in suspended load of the Mackenzie River. In addition, our end member mixing analysis allows us to provide the first estimates of [OC<sub>biosphere</sub>], which varies between  $0.7 \pm 0.1\%$  and  $2.4 \pm 0.2\%$ . To estimate POC<sub>biosphere</sub> discharge, we use the most complete dataset of annual sediment discharge to the Mackenzie Delta (1974-1994)<sup>15</sup>, which ranged from  $81 \text{ Tg yr}^{-1}$  to  $224 \text{ Tg yr}^{-1}$ . A Monte Carlo approach is used to account for the modest sample size by using the full measured variability in both [OC<sub>biosphere</sub>] and sediment discharge (Methods). We estimate POC<sub>biosphere</sub> discharge =  $2.2_{-0.9}^{+1.3} \text{ TgC yr}^{-1}$  which is sustainable over  $10^3$ - $10^4$  years, depleting the soil carbon stock by  $\sim 0.006\% \text{ yr}^{-1}$  (Methods). We estimate the POC<sub>petro</sub> discharge =  $0.4_{-0.1}^{+0.1}$ . These estimates do not account for ice covered conditions when <10% of the annual sediment discharge is conveyed<sup>12</sup>. Nevertheless, our estimate of POC<sub>biosphere</sub> discharge is greater than the combined POC discharge of  $\sim 1.9 \text{ TgC yr}^{-1}$  by the major Eurasian Arctic Rivers (Ob, Yenisei, Lena, Indigirka and Koyma)<sup>11,27</sup> which cover  $\sim 8.6 \times 10^6 \text{ km}^2$ . Based on the available measurements, the Mackenzie River dominates the input of POC<sub>biosphere</sub> to the Arctic Ocean.

The mobilisation of millennial-aged POC<sub>biosphere</sub> from soils at high latitudes has been viewed as a short-term source to the atmosphere if decomposition releases greenhouse gases (CH<sub>4</sub> and CO<sub>2</sub>)<sup>2-6,8</sup>. However, if POC<sub>biosphere</sub> escapes oxidation during river transport and is buried offshore, erosion acts as a long-term CO<sub>2</sub> sink<sup>10,18,20</sup>. Offshore, aged POC<sub>biosphere</sub> from the Mackenzie River (Fig. 1) can explain the <sup>14</sup>C depletion and δ<sup>13</sup>C of bulk organic matter, and old <sup>14</sup>C ages of terrestrial plant wax compounds (up to 20,000 yr) in surface sediments of the Beaufort Sea<sup>7,28,29</sup>. We provide new evidence that terrestrial POC is buried efficiently offshore and accumulates in sediments over  $10^4$  years. Benthic foraminifera <sup>14</sup>C ages in a borehole located at the head of the Mackenzie Trough (MTW01) indicates that 21m of

150 sediment have accumulated since  $9183^{+125}_{-156}$  cal. yr BP, suggesting a high sedimentation rate  
151 during the Holocene  $2.7 \pm 0.1$  m ka<sup>-1</sup> (Extended Data Table 2, Methods). These marine  
152 sediments have [OC<sub>total</sub>] values similar to those measured in the Mackenzie River in both the  
153 <63μm (1.5% to 1.7%) and >63μm (1.1% to 1.4%) size fractions (Fig. 3). Their N/OC<sub>total</sub> and  
154 δ<sup>13</sup>C<sub>org</sub> values suggest that they are dominated by terrestrial POC with minor marine OC  
155 addition (Extended Data Fig. 5). We use the change in OC<sub>total</sub>/Al ratios offshore to estimate  
156 OC burial efficiencies have been  $65 \pm 27\%$  or more over the Holocene at this site (Methods).  
157 Rapid sediment accumulation and low temperature are likely to promote high POC burial  
158 efficiency<sup>18,23,28</sup>. Also, the fluvial transport dynamics of POC<sub>biosphere</sub> may promote burial (Fig.  
159 2c). The oldest, most-degraded POC<sub>biosphere</sub> is transported with clays<sup>25</sup>, whose association  
160 with organic matter may enhance burial efficiency<sup>18</sup>, while the youngest, least-degraded  
161 POC<sub>biosphere</sub> is carried near the river bed at the highest sediment concentrations. Our findings  
162 suggest that erosion and riverine transfer at high latitudes can lead to the long-term  
163 preservation of terrestrial POC in marine sediments (Fig. 3).

164 Erosion of high latitude soils and riverine export of POC<sub>biosphere</sub> may represent an  
165 important geological CO<sub>2</sub> sink. Our estimate of the modern day POC<sub>biosphere</sub> discharge of  
166  $2.2^{+1.3}_{-0.9}$  TgC yr<sup>-1</sup> in the Mackenzie River may be refined by additional temporal sampling.  
167 However, it is three times the modern rates of CO<sub>2</sub> drawdown by weathering of silicate  
168 minerals by carbonic acid in the Mackenzie River<sup>16</sup>, at ~0.7 TgC yr<sup>-1</sup>. Preservation of POC  
169 offshore (Fig. 3) suggests that erosion of high latitude soils, riverine POC<sub>biosphere</sub> transport and  
170 export to the ocean acts as the largest geological CO<sub>2</sub> sink operating in the Mackenzie Basin.  
171 It is important to note that these longer-term fluxes are lower than estimates of greenhouse  
172 gas emissions from high latitude soils in permafrost zones due to projected warming over the  
173 coming century<sup>3,5,6,30</sup>. While these fluxes remain uncertain, recent work<sup>30</sup> has proposed  
174 emissions of ~ 1–2 PgC yr<sup>-1</sup> which equate to a yield of ~70 tC km<sup>-2</sup> yr<sup>-1</sup> over  $17.8 \times 10^8$  km<sup>2</sup> of

175 soils in permafrost zones. This estimate of accelerated release of CO<sub>2</sub> due to anthropogenic  
176 warming<sup>30</sup> is more rapid than the natural geological drawdown fluxes, of which we estimate  
177 POC<sub>biosphere</sub> ~ 2–5 tC km<sup>-2</sup> yr<sup>-1</sup> for the Mackenzie Basin (Methods). Over longer-time periods,  
178 we postulate that this geological CO<sub>2</sub> sink may be sensitive to climate conditions in the  
179 Arctic. The carbon transfer can operate when high latitudes host significant POC<sub>biosphere</sub>  
180 stocks in soil, and while rivers can erode and transfer sediments to the Arctic Ocean. Over the  
181 last 1Ma, the POC<sub>biosphere</sub> transfer was likely to have been enhanced during interglacials<sup>24</sup>  
182 (Fig. 3), whereas during glacial conditions, lower soil POC<sub>biosphere</sub> stocks and extensive ice-  
183 sheet coverage suggest that POC<sub>biosphere</sub> erosion may have been suppressed. We propose that  
184 erosion of terrestrial POC<sub>biosphere</sub> by large rivers draining the Arctic could play an important  
185 role in long-term CO<sub>2</sub> drawdown<sup>19,20</sup>, coupling the carbon cycle to climatic conditions at high  
186 latitudes.

187 **References:**

- 188 1. Gorham, E. Northern peatlands: Role in the carbon cycle and probable responses to  
189 climatic warming. *Ecological Applications* **1**, 182–195 (1991).
- 190 2. Tarnocai, C. *et al.* Soil organic carbon pools in the northern circumpolar permafrost  
191 region. *Global Biogeochemical Cycles* **23**, GB2023 (2009).
- 192 3. Schuur, E. A. G. *et al.* Vulnerability of permafrost carbon to climate change:  
193 Implications for the global carbon cycle. *Bioscience* **58**, 701–714 (2009).
- 194 4. Guo, L., Ping, C.-L., & Macdonald, R. W. Mobilization pathways of organic carbon  
195 from permafrost to arctic rivers in a changing climate. *Geophysical Research Letters* **34**,  
196 L13603 (2007).
- 197 5. MacDougall, A. H., Avis, C. A, & Weaver, A. L. Significant contribution to climate  
198 warming from the permafrost carbon feedback. *Nature Geoscience* **5**, 719–721 (2012).

- 199 6. Schädel, C. *et al.* Circumpolar assessment of permafrost C quality and its vulnerability  
200 over time using long-term incubation data. *Global Change Biology* **20**, 641–652 (2014).
- 201 7. Goñi, M. A., Yunker, M. B., Macdonald, R. W., & Eglinton, T.I. The supply and  
202 preservation of ancient and modern components of organic carbon in the Canadian  
203 Beaufort Shelf of the Arctic Ocean. *Marine Chemistry* **93**, 53–73 (2005).
- 204 8. Vonk, J. E. *et al.* Activation of old carbon by erosion of coastal and subsea permafrost  
205 in Arctic Siberia. *Nature* **489**, 137–140 (2012).
- 206 9. Vonk, J. E., & Gustafsson, O. Permafrost-carbon complexities. *Nature Geoscience* **6**,  
207 675–676 (2013).
- 208 10. Galy, V. *et al.* Efficient organic carbon burial in the Bengal fan sustained by the  
209 Himalayan erosional system. *Nature* **450**, 407–410 (2007).
- 210 11. Stein, R., & Macdonald, R. W. *The Organic Carbon Cycle in the Arctic Ocean*  
211 Springer, Berlin (2004).
- 212 12. Macdonald, R.W. *et al.* A sediment and organic carbon budget for the Canadian  
213 Beaufort Shelf. *Marine Geology* **144**, 255–273 (1998).
- 214 13. Galy, V., & Eglinton, T. I. Protracted storage of biospheric carbon in the Ganges-  
215 Brahmaputra basin. *Nature Geoscience* **4**, 843–847 (2011).
- 216 14. Bouchez, J. *et al.* Source, transport and fluxes of Amazon River particulate organic  
217 carbon: Insights from river sediment depth-profiles. *Geochimica et Cosmochimica Acta*  
218 **133**, 280–298 (2014).
- 219 15. Carson, M. A., Jasper, J. N., & Conly, F.M. Magnitude and sources of sediment input to  
220 the Mackenzie Delta, Northwest Territories, 1974–94. *Arctic* **51**, 116–124 (1998).
- 221 16. Gaillardet, J., Dupré, B., Louvat, P., & Allegre, C. A. Global silicate weathering and  
222 CO<sub>2</sub> consumption rates deduced from the chemistry of large rivers. *Chemical Geology*  
223 **159**, 3–30 (1999).

- 224 17. Sundquist, E.T., & Visser, K. The geologic history of the carbon cycle. In Schlesinger,  
225 W.H., ed., *Treatise on Geochemistry*, Volume 8, Biogeochemistry: Oxford, UK,  
226 Elsevier-Pergamon, 425–472 (2004).
- 227 18. Blair, N. E. & Aller, R. C. The fate of terrestrial organic carbon in the marine  
228 environment, *Annual Review of Marine Sciences* **4**, 17.1–17.23 (2012).
- 229 19. Hayes, J. M., Strauss, H. & Kaufman, A. J. The abundance of  $^{13}\text{C}$  in marine organic  
230 matter and isotopic fractionation in the global biogeochemical cycle of carbon during  
231 the past 800 Ma. *Chemical Geology* **161**, 103–125 (1999).
- 232 20. Berner, R. A. Atmospheric CO<sub>2</sub> levels over Phanerozoic time. *Science* **249**, 1382–1386  
233 (1990).
- 234 21. Hilton, R. G., Gaillardet, J., Calmels, D., & Birck, J. L. Geological respiration of a  
235 mountain belt revealed by the trace element rhenium. *Earth and Planetary Science  
Letters* **403**, 27–36 (2014).
- 237 22. Hilton, R. G. *et al.* Climatic and geomorphic controls on the erosion of terrestrial  
238 biomass from subtropical mountain forest. *Global Biogeochemical Cycles* **26**, 3,  
239 doi:10.1029/2012GB004314 (2012).
- 240 23. Burdige, D. J. Burial of terrestrial organic matter in marine sediments: A re-assessment.  
241 *Global Biogeochemical Cycles* **19**, GB4011 1–7 (2005).
- 242 24. MacDonald, G. M. *et al.* Rapid development of the circumarctic peatland complex and  
243 atmospheric CH<sub>4</sub> and CO<sub>2</sub> variations. *Science* **314**, 285–288 (2006).
- 244 25. Dellinger, M. *et al.* Lithium isotopes in large rivers reveal the cannibalistic nature of  
245 modern continental weathering and erosion. *Earth and Planetary Science Letters* **401**,  
246 359–372 (2014).
- 247 26. Kuhry, P., & Vitt, D. H. Fossil carbon/nitrogen ratios as a measure of peat  
248 decomposition. *Ecology* **77**, 271–275 (1996).

- 249 27. Feng, X. *et al.* Differential mobilization of terrestrial carbon pools in Eurasian Arctic  
250 river basins. *Proceedings of the National Academy of Sciences USA* **110**, 14168–14173  
251 (2013).
- 252 28. Goñi, M. A. *et al.* Distribution and sources of organic matter in surface marine  
253 sediments across the North American Arctic margin. *Journal of Geophysical Research -*  
254 *Oceans* **118**, 4017–4035 (2013).
- 255 29. Drenzek, N. J., Montluçon, D. B., Yunker, M. B., Macdonald, R. W., & Eglinton, T. I.  
256 Constraints on the origin of sedimentary organic carbon in the Beaufort Sea from  
257 coupled molecular  $^{13}\text{C}$  and  $^{14}\text{C}$  measurements. *Marine Chemistry* **103**, 146–162 (2007).
- 258 30. Schuur, E. A. G. *et al.* Climate change and the permafrost carbon feedback. *Nature* **520**,  
259 171–179 (2015).

260 **Acknowledgements:** Radiocarbon measurements were funded by the Natural Environment  
261 Research Council (NERC), UK (Allocation 1611.0312) to R.G.H and C.B. Fieldwork was  
262 funded by CNRS (OXYMORE and CANNIBALT) to J.G. and R.G.H., the Woods Hole  
263 Oceanographic Institution Arctic Research Initiative to V.G. and an Early Career Research  
264 Grant by the British Society for Geomorphology to R.G.H. V.G. was supported by the US  
265 National Science Foundation (OCE-0928582) and H.C. by a Royal Society University  
266 Fellowship. The research was carried out under Scientific Research Licence No. 14802 issued  
267 by the Aurora Research Centre, who we thank for logistical support (in particular D. Ross  
268 and J. Gareis). Thanks to I. Peters for preparation of offshore borehole samples. E. Tipper and  
269 K. Hilton are thanked for field assistance and discussions and D. Ofukany, G. Lennie, R.  
270 Wedel and R. Pilling of Environment Canada for loan of equipment. Three anonymous  
271 reviewers are thanked for thoughtful comments which improved the manuscript.

272 **Author Contributions:** R.G.H., V.G. and J.G. conceived the study and R.G.H., J.B., D.C.,  
273 V.G. and M.D. designed the fieldwork and collected the river samples. M.O. and H.C.

274 collected sediment and carbonate data from the offshore borehole. R.G.H., V.G., M.D., C.B.  
275 and D.G. processed the samples and carried out the geochemical analyses. R.G.H. wrote the  
276 manuscript with input from all co-authors.

277 **Author Information:** Data are found in the Extended Data Tables. Reprints and permissions  
278 information is available at [www.nature.com/reprints](http://www.nature.com/reprints). The authors declare they have no  
279 competing financial interests. Correspondence and requests for materials should be addressed  
280 to [r.g.hilton@durham.ac.uk](mailto:r.g.hilton@durham.ac.uk).

281 **Figure Legends**

282 **Figure 1: Source of particulate organic carbon (POC) in the Mackenzie River Basin.**  
283 Radiocarbon activity of POC ( $F_{\text{mod}}$ ) versus the nitrogen to organic carbon ratio ( $\text{N}/\text{OC}_{\text{total}}$ ) of  
284 sediments from the Mackenzie River (circles) at the delta (black), Tsiigehtchic (grey) and  
285 Norman Wells (white) and major tributaries the Liard (diamond), Peel (dark blue square) and  
286 Arctic Red (light blue square). River depth profiles collected in 2010 and 2011 suspended  
287 load (filled symbols), river bed materials (open symbols) and sieved bank samples (2009) are  
288 shown with analytical errors (2 s.d.) as grey lines if larger than points. The dashed line shows  
289 the compositions expected by mixing rock-derived, petrogenic POC ( $\text{POC}_{\text{petro}}$ ) and biospheric  
290 POC ( $\text{POC}_{\text{biosphere}}$ ). Solid green line is the trend from a peat core in western Canada<sup>26</sup>.

291 **Figure 2: Transport of particulate organic carbon (POC) in the Mackenzie River. a.**  
292 River depth profile collection from the Mackenzie River Delta during falling stage, with  
293 Acoustic Doppler Current Profiler data to determine channel geometry, water velocity and  
294 water discharge ( $\text{m}^3 \text{s}^{-1}$ ). **b.** Aluminium to Silicon ratio (Al/Si, molar), a proxy for sediment  
295 grain size<sup>25</sup>, with water depth normalised to maximum depth. Coarser materials are carried  
296 throughout the profile during high stage. **c.** Radiocarbon activity of POC ( $F_{\text{mod}}$ ) versus Al/Si  
297 for the Mackenzie Basin (this study, symbols as Fig. 1), Amazon River<sup>14</sup>, and Ganges

298 River<sup>10,13</sup>. River suspended load (filled) and river bed materials (open) are distinguished with  
299 analytical errors (2 s.d.) shown as grey lines if larger than points.

300 **Figure 3: Fate of particulate organic carbon offshore.** **a.** Organic carbon concentration  
301 ( $[OC_{total}]$ , %) of suspended sediments in the Mackenzie River Delta (n=8) where solid line  
302 and grey box show the mean  $\pm$  standard error, whiskers show  $\pm$  standard deviation and the  
303 circles indicate the minimum and maximum values. **b.**  $[OC]_{total}$  in sediments  $<63\mu m$  and  
304  $>63\mu m$  from core MTW01 in the Mackenzie Trough (Extended Data Fig. 1) for depths dated  
305 by the  $^{14}C$  activity of mixed benthic foraminifera (Methods), where whiskers show analytical  
306 error if large than the point size.

307 **Methods**

308 **River sample collection and preparation:** River depth-profiles from September 2010 and  
309 June 2011 (Extended Data Table 1) were used to collect the full range of erosion products  
310 and POC in large river systems, taking advantage of the hydrodynamic sorting of  
311 particles<sup>10,13,14,25</sup>. At each sampling site (Fig. 1) channel depth, water velocity and  
312 instantaneous water discharge were measured by two or more transects with an Acoustic  
313 Doppler Current Profiler (ADCP Rio Grande 600 kHz) before each depth profile was  
314 collected at a single point ( $\pm 10m$ ) in the middle of the channel. On the boat, each sample (~7-  
315 8L) was evacuated into a clean bucket and stored in sterilised plastic bags and the procedure  
316 repeated depending upon the total water depth. Each bag was weighed to determine the  
317 sampled volume, then the entire sample was filtered within 24 hrs through pre-cleaned Teflon  
318 filter units through 90 mm diameter  $0.2\mu m$  PES filters<sup>13,25</sup>. Suspended sediment was  
319 immediately rinsed from the filter using filtered river water into clean amber-glass vials and  
320 kept cool. River bed materials were collected at the base of the depth transects from the boat,  
321 using a metal bucket as a dredge, and decanted to a sterile bag. River bank deposits (June

322 2009) were collected from fresh deposits close to the channel (Extended Data Table 3) and  
323 sieved at 250 µm and 63 µm to investigate the sorting of POC<sup>31</sup>. All sediments were freeze  
324 dried upon return to laboratories within 2 weeks, weighed and homogenised in an agate  
325 grinder.

326 **Offshore borehole sampling and benthic foraminifera sample preparation:** Benthic  
327 foraminifera-containing marine sediment samples were obtained from the upper 22 m  
328 Holocene sequence of an 85.1 m MTW01 borehole<sup>32</sup> located at 69° 20' 53" N, 137° 59' 13"  
329 in 45 m water depth in the Mackenzie Trough (Extended Data Fig. 1). Drilled by the  
330 Geological Survey of Canada in 1984, the core is currently archived at the GSC-Atlantic core  
331 repository. To isolate foraminifera, sediment samples were disaggregated over a <38µm mesh  
332 sieve using deionized water. Based on down-hole microfossils counts, 4 samples were  
333 selected with sufficient specimens for radiocarbon dating.

334 **Geochemical analyses:** For the river suspended sediments and core samples for organic  
335 carbon analyses, inorganic carbon was removed using a HCl fumigation technique to avoid  
336 loss of a component of POC which is known to occur during a HCl leach<sup>33</sup>. An adapted  
337 method to ensure full removal of detrital dolomite was used<sup>34</sup>. In summary, samples were  
338 placed in an evacuated desiccator containing ~50 ml 12N HCl in an oven at between 60 and  
339 65 °C for 60 to 72 hours. Sample were then transferred to another vacuum desiccator charged  
340 with indicating silica gel, pumped down again and dried to remove HCl fumes. River  
341 sediment samples were analysed for organic carbon concentration [OC<sub>total</sub>] on acidified  
342 aliquots and nitrogen concentration ([N], %) on non-acidified aliquots by combustion at  
343 1020°C in O<sub>2</sub> using a Costech elemental analyser (EA) in Durham. For river depth profile  
344 samples, acidified aliquots were prepared to graphite at the NERC Radiocarbon Facility of  
345 between 1-2 mg C for each sample and standard and <sup>14</sup>C was measured by Accelerator Mass  
346 Spectrometry at the Scottish Universities Environmental Research Centre and reported as

347 fraction modern ( $F_{\text{mod}}$ ) by standard protocol<sup>35</sup>. Process standards (96H humin) and  
348 background materials (bituminous coal) were taken through all stages of sample preparation  
349 and  $^{14}\text{C}$  analysis and were within  $2\sigma$  uncertainty of expected values. Stable isotopes of POC  
350 ( $\delta^{13}\text{C}_{\text{org}}$ ) were measured by dual-inlet isotope ratio mass spectrometer (IRMS) on an aliquot  
351 of the same  $\text{CO}_2$ . These measurements were consistent with  $\delta^{13}\text{C}_{\text{org}}$  measurements made by  
352 EA-IRMS normalised based on measured values standards ( $n=7$ ) spanning  $>30\text{\textperthousand}$  and long-  
353 term analytical precision of  $0.2\text{\textperthousand}$ . River bank samples from 2009 were analysed by similar  
354 procedures at the National Ocean Sciences Accelerator Mass Spectrometry Facility  
355 (NOSAMS) at Woods Hole Oceanographic Institution.

356 Mixed benthic foraminifera samples picked from the MTW01 core were analysed at  
357 NOSAMS for  $^{14}\text{C}$  analyses. Samples were rinsed and no pre-treatments were used. The  
358 samples were directly hydrolyzed with strong acid,  $\text{H}_3\text{PO}_4$ , to convert the carbon in the  
359 sample to  $\text{CO}_2$ . Calibration of the  $^{14}\text{C}$  dates was performed using CALIB (version 7.1)<sup>36</sup>. All  
360  $^{14}\text{C}$  dates were normalized to a  $\delta^{13}\text{C}$  of  $-25\text{\textperthousand}$  versus VPDB (<http://intcal.qub.ac.uk/calib/>).  
361 Foraminifera dates were calibrated using the MARINE13 dataset<sup>37</sup>, with a reservoir age  
362 correction ( $\Delta R$ ) of  $335 \pm 85$  yrs (Extended Data Table 2). The  $\Delta R$  value is based on a recent  
363 re-analysis of ages from 24 living molluscs collected before 1956 from the northwestern  
364 Canadian Arctic Archipelago<sup>38</sup>. This calibration set does not include specimens from the  
365 Beaufort Sea and as such provides only a best available estimate for  $\Delta R$  in the Mackenzie  
366 Trough.

367 **End member mixing model:** The  $F_{\text{mod}}$ ,  $\text{N}/\text{OC}_{\text{total}}$  (Fig. 1),  $\delta^{13}\text{C}_{\text{org}}$  values and  $\text{Al}/\text{OC}_{\text{total}}$   
368 values (Extended Data Fig. 2) are consistent with a mixing of  $\text{POC}_{\text{petro}}$  and  $\text{POC}_{\text{biosphere}}$   
369 dominating the bulk geochemical composition of river POC. Autochthonous sources are not  
370 significant based on those measured values, which is consistent with the turbid nature of the  
371 Mackenzie River (mean suspended sediment concentration of  $\sim 300\text{--}400$  mg/L) meaning that

372 like other turbid river systems (e.g. the Ganges-Brahmaputra) light penetration is minimal. A  
373 mixture of  $\text{POC}_{\text{petro}}$  and  $\text{POC}_{\text{biosphere}}$  can be described by governing equations<sup>10,13,31</sup>:

374  $f_{\text{biosphere}} + f_{\text{petro}} = 1$  (Equation 1)

375  $f_{\text{biosphere}} \times \theta_{\text{biosphere}} + f_{\text{petro}} \times \theta_{\text{petro}} = \theta_{\text{sample}}$  (Equation 2)

376 where  $f_{\text{biosphere}}$  and  $f_{\text{petro}}$  are the fractions of POC derived from biospheric and petrogenic  
377 sources, respectively.  $\theta_{\text{sample}}$  is the measured composition (e.g.  $F_{\text{mod}}$ ) of a river POC sample,  
378 and  $\theta_{\text{biosphere}}$  and  $\theta_{\text{petro}}$  are the compositions of biospheric and petrogenic sources. To quantify  
379 the  $f_{\text{petro}}$  in each sample we use the aluminium (Al) to  $\text{OC}_{\text{total}}$  concentration ratio in river  
380 sediments. At each locality, a linear trend between  $F_{\text{mod}}$  and Al/ $\text{OC}_{\text{total}}$  (Extended Data Fig.  
381 2b) can be explained by a mixture of an Al-rich, OC-poor material (rock fragments  
382 containing  $\text{POC}_{\text{petro}}$ ) with Al-poor, OC-rich material (soils and vegetation debris as  
383  $\text{POC}_{\text{biosphere}}$ ). Taking advantage of the fact that the  $\text{POC}_{\text{petro}}$  has  $F_{\text{mod}} \sim 0$ , the intercept at  $F_{\text{mod}} =$   
384 0 gives an estimate of the Al/ $\text{OC}_{\text{total}}$  values and associated uncertainty of the sedimentary  
385 rock end member. To estimate the average concentration of  $\text{OC}_{\text{petro}}$  of bedrocks in each basin  
386 ( $[\text{OC}_{\text{petro}}]$ , %), we use the Al concentration of river bed materials as a proxy of for the Al  
387 concentration in the bedrocks<sup>25</sup> and the Al/ $\text{OC}_{\text{total}}$  value at  $F_{\text{mod}} \sim 0$ . Following previous work  
388 in large rivers, we then assume that the  $\text{OC}_{\text{petro}}$  is well mixed in the water column and has a  
389 relatively constant  $[\text{OC}_{\text{petro}}]$  (refs 10,13,14). This method may overestimate  $f_{\text{petro}}$  if  $\text{OC}_{\text{petro}}$  has  
390 been more extensively oxidised in fine grained weathering products carried in the suspended  
391 load<sup>21</sup>.  $f_{\text{petro}}$  is quantified using  $[\text{OC}_{\text{petro}}]$  and measured  $[\text{OC}_{\text{total}}]$ .

392 The mixing analysis returns a  $[\text{OC}_{\text{petro}}] = 0.12 \pm 0.03\% (\pm 2\sigma)$  in the Liard River and  
393 Mackenzie River at Tsiigehtchic, higher values in the Peel River  $[\text{OC}_{\text{petro}}] = 0.63 \pm 0.30\%$ ,  
394 with the Mackenzie River at the delta with an intermediate value  $[\text{OC}_{\text{petro}}] = 0.29 \pm 0.05\%$ .  
395 This is consistent with the known presence of  $\text{POC}_{\text{petro}}$ -bearing sedimentary rocks in the

396 Mackenzie River Basin and high OC<sub>total</sub> contents of bedrocks in the upper Peel River Basin  
397 and Mackenzie mountains<sup>39</sup>. To quantify the average <sup>14</sup>C age of POC<sub>biosphere</sub> in each sample,  
398 Equations 1 and 2 can be solved for  $\theta_{biosphere}$ , using the  $f_{petro}$  and assumed unmeasurable above  
399 background <sup>14</sup>C content of POC<sub>petro</sub> ( $F_{mod} = 0$ ). The uncertainty mainly derives from that on  
400  $f_{petro}$  and [OC<sub>total</sub>] and has been propagated through the calculations.

401 To test if the mixing of POC<sub>biosphere</sub> and POC<sub>petro</sub> can describe the composition of the  
402 suspended load samples, we predict the  $\delta^{13}\text{C}_{org}$  measurements which were not used in the  
403 mixing analysis. The calculated  $f_{petro}$  values and end member values of -26.2±0.5‰ for  
404 POC<sub>biosphere</sub> and -28.6±0.5‰ for POC<sub>petro</sub> were used, informed by measurements of  
405 bedrocks<sup>39</sup> and vegetation and soil in the basin<sup>40</sup>. The mixing model (equation 2) can robustly  
406 predict the  $\delta^{13}\text{C}_{org}$  differences between the Peel and Liard rivers, and between suspended load  
407 and bed material  $\delta^{13}\text{C}_{org}$  values (Extended Data Fig. 2c), supporting a mixing control on the  
408 variables.

409 **Mackenzie River POC discharge:** To quantify the discharge of POC we need to account for  
410 the variability in suspended sediment discharge and the variability in the POC<sub>biosphere</sub> and  
411 POC<sub>petro</sub> content of sediments in the basin. We use the longest, most complete quantification  
412 of sediment flux by the Mackenzie River from 1974-1994<sup>15</sup>, which has an average 127±40 Tg  
413 yr<sup>-1</sup> ( $\pm 1\sigma$ ). Annual sediment yield varied from 81 Tg yr<sup>-1</sup> to 224 Tg yr<sup>-1</sup>. While the POC  
414 samples were not collected at the same time period, our measurements of [OC<sub>total</sub>] at the  
415 Delta, mean = 1.6±0.5% (n=8,  $\pm 1\sigma$ ) and do not vary systematically between falling and high  
416 stage (Extended Data Fig. 4) and are consistent with available data from samples<sup>12</sup> collected  
417 in 1987 (1.4±0.2, n=10). While future work should aim to constrain the variability in POC  
418 composition further, these observations suggest that temporal variability may be less  
419 important than the potential variability in [OC<sub>total</sub>] with depth at a given time, where we find  
420 [OC<sub>total</sub>] values can range from 1.0% to 2.7%. We use our measured range of [OC<sub>biosphere</sub>] and

[OC<sub>petro</sub>] values and the full range of annual sediment yields<sup>15</sup> to quantify POC<sub>biosphere</sub> and POC<sub>petro</sub> discharge and associated uncertainty using a Monte Carlo approach. Over 100,000 simulations, we use a ‘flat’ probability for the range of values for both variables (i.e. equal probability of all measured values). This allows us to fully explore the range of estimates given the available measurements. Future work seeking to expand the number of [OC<sub>biosphere</sub>] measurements to assess its flux-weighted mean and variability, while assessing temporal variability in more detail, will allow POC discharge estimates and their uncertainty to be refined. POC<sub>biosphere</sub> ( $2.2_{-0.9}^{+1.3}$  TgC yr<sup>-1</sup>) and POC<sub>petro</sub> ( $0.4_{-0.1}^{+0.1}$ ) discharges are reported as the median (50%)  $\pm$  1 s.d. Over the sediment source areas of the Mackenzie (Downstream of the Great Slave Lake<sup>15</sup>) of 774,200 km<sup>2</sup>, these equate to yields of POC<sub>biosphere</sub> =  $2.9_{-1.1}^{+1.7}$  tC km<sup>-2</sup> yr<sup>-1</sup> and POC<sub>petro</sub> =  $0.6_{-0.2}^{+0.2}$  tC km<sup>-2</sup> yr<sup>-1</sup>. The total POC discharge is slightly higher than a previous estimate (2.1 TgC yr<sup>-1</sup>)<sup>12</sup> based on measurements of POC content made in 1987 because we: i) account for higher POC<sub>biosphere</sub> concentrations which may occur in water-logged POC<sub>biosphere</sub> near the river bed (Figs. 2c, Extended Data Fig. 4); and ii) account for the potential for very high annual sediment discharge<sup>15</sup>. Based on estimates of soil carbon stock in the Mackenzie Basin<sup>2</sup> of  $\sim 50 \times 10^3$  tC km<sup>-2</sup> and the upstream sediment source area (downstream of the Great Slave Lake, 774,200 km<sup>2</sup>), the present rate of POC<sub>biosphere</sub> export represents a depletion of the soil carbon stock by  $\sim 0.006\%$  yr<sup>-1</sup>, which is sustainable over  $10^3$ - $10^4$  years.

**OC burial efficiency in MTW01:** To estimate the burial efficiency of terrestrial POC at the MTW01 site, we normalise the measured [OC<sub>total</sub>] concentrations (Fig. 3) by Al concentration, an immobile inorganic element hosted by major mineral phases. The OC<sub>total</sub>/Al normalization allows the effects of dilution to be distinguished from net OC gain (increased ratio) or OC loss (decreased ratio). The mean OC<sub>total</sub>/Al of the MTW01 samples was  $0.17 \pm 0.02$  (g g<sup>-1</sup>, n=4,  $\pm 2SE$ ). This is lower than the mean OC<sub>total</sub>/Al of the suspended load

samples from the Mackenzie River delta of  $0.26 \pm 0.10$  ( $\text{g g}^{-1}$ ,  $n=8$ ,  $\pm 2\text{SE}$ ). The decrease in the ratio offshore may suggest a higher relative proportion of  $\text{POC}_{\text{petro}}$  (Extended Data Fig. 2b), however this is not consistent with the less negative  $\delta^{13}\text{C}_{\text{org}}$  values (Extended Data Fig. 5). The decrease can therefore be interpreted in terms of OC loss, with the ratio of core to river samples ( $0.17 \pm 0.02$  /  $0.26 \pm 0.10$ ). Assuming that all the change in  $\text{OC}_{\text{total}}/\text{Al}$  is driven by OC loss, and taking into account the measurement variability in these values, we estimate that  $65 \pm 27\%$  of the OC has been preserved. However, we note that the  $\text{OC}_{\text{total}}/\text{Al}$  ratios in the core are not statistically different from the river suspended load samples (one-way ANOVA,  $P > 0.1$ ) which suggest the OC burial efficiency could be higher (i.e. 100%). In addition, if we use the  $\text{OC}_{\text{total}}/\text{Al}$  of finer river sediments carried near the channel surface which may be more easily conveyed offshore of  $0.20 \pm 0.04$  ( $\text{g g}^{-1}$ ,  $n=4$ ,  $\pm 2\text{SE}$ ), we calculate burial efficiency =  $85 \pm 20\%$ . Future work should seek to better constrain these burial efficiencies with additional terrestrial and marine samples. Nevertheless, despite the remaining uncertainty, these high burial efficiencies<sup>18</sup> are consistent with the high sedimentation rate and low temperature setting. The long-term burial of POC delivered to sites deeper in the Beaufort Sea<sup>28</sup> still remains to be assessed, in order to provide a complete picture of source to sink carbon transfers.

**Methods references:**

31. Hilton, R.G., Galy, A., Hovius, N., Horng, M. J., & Chen, H. The isotopic composition of particulate organic carbon in mountain rivers of Taiwan. *Geochimica et Cosmochimica Acta* **74**, 3164–3181 (2010).
32. Moran, K., Hill, P.R., & Blasco, S.M. Interpretation of piezocone penetrometer profiles in sediment from the Mackenzie Trough, Canadian Beaufort Sea. *Journal of Sedimentary Petrology* **59**, 88–97 (1989).

- 470 33. Komada, T., Anderson, M. R., & Dorfmeier, C. L. Carbonate removal from coastal  
471 sediments for the determination of organic carbon and its isotopic signatures,  $^{13}\text{C}$  and  
472  $^{14}\text{C}$ : Comparison of fumigation and direct acidification by hydrochloric acid. *Limnology*  
473 and *Oceanography* **6**, 254–262 (2008).
- 474 34. Whiteside, J. H. *et al.* Pangean great lake paleoecology on the cusp of the end-Triassic  
475 extinction. *Palaeogeography, Palaeoclimatology, Palaeoecology* **301**, 1–17 (2011).
- 476 35. Stuiver, M., & Polach H. A. Discussion: Reporting of  $^{14}\text{C}$  data. *Radiocarbon* **19**, 55–63  
477 (1977).
- 478 36. Stuiver, M., & Reimer, P. J. Extended  $^{14}\text{C}$  database and revised CALIB radiocarbon  
479 calibration program, *Radiocarbon* **35**, 215-230 (1993)
- 480 37. Reimer, P. J. *et al.* IntCal09 and Marine09 Radiocarbon Age Calibration Curves, 0–  
481 50,000 Years cal BP. *Radiocarbon* **51**, 1111-1150 (2009)
- 482 38. Coulthard, R. D., Furze, M. F. A., Pienkowski, A. J., Nixon, F. C. & England, J. H. New  
483 marine  $\Delta\text{R}$  values for Arctic Canada. *Quaternary Geochronology* **5**, 419–434 (2010).
- 484 39. Johnston, D. T., Macdonald, F. A., Gill, B.C., Hoffman, P. F., & Schrag, D. P.  
485 Uncovering the Neoproterozoic carbon cycle. *Nature* **483**, 320–323 (2012).
- 486 40. Bird, M., Santruckova, H., Lloyd, J., & Lawson, E. The isotopic composition of soil  
487 organic carbon on a north-south transect in western Canada. *European Journal of Soil  
488 Science* **53**, 393–403 (2002).
- 489 41. Brown, J. *et al.* *Circum-arctic map of permafrost and ground ice conditions*. National  
490 Snow and Ice Data Center/World Data Center for Glaciology, Boulder, CO. (1998).

491 **Extended Data**

492 Available by contacting the lead author ([r.g.hilton@durham.ac.uk](mailto:r.g.hilton@durham.ac.uk)) or on the online version of  
493 the paper: doi:10.1038/nature14653.

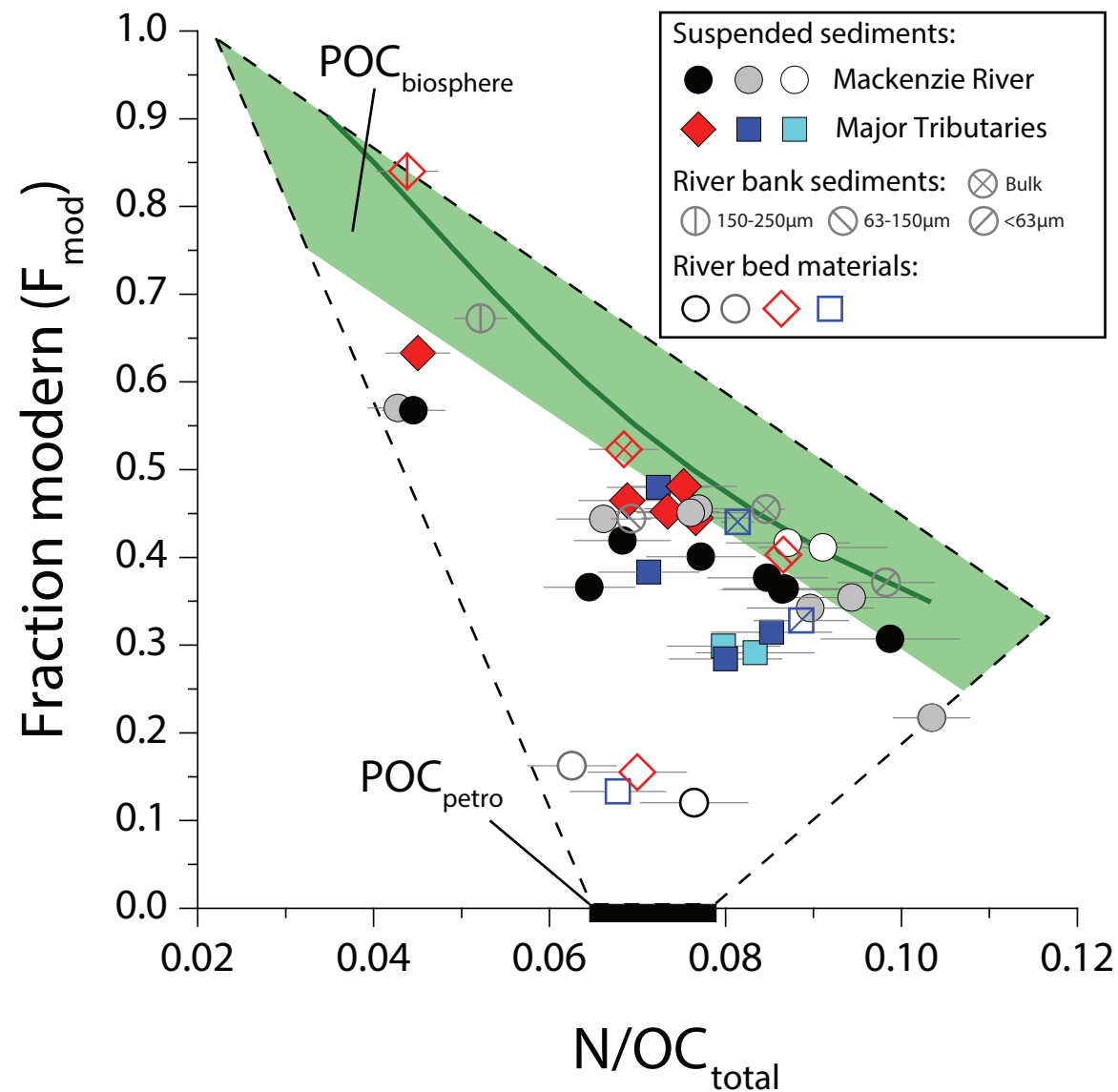


Figure 1

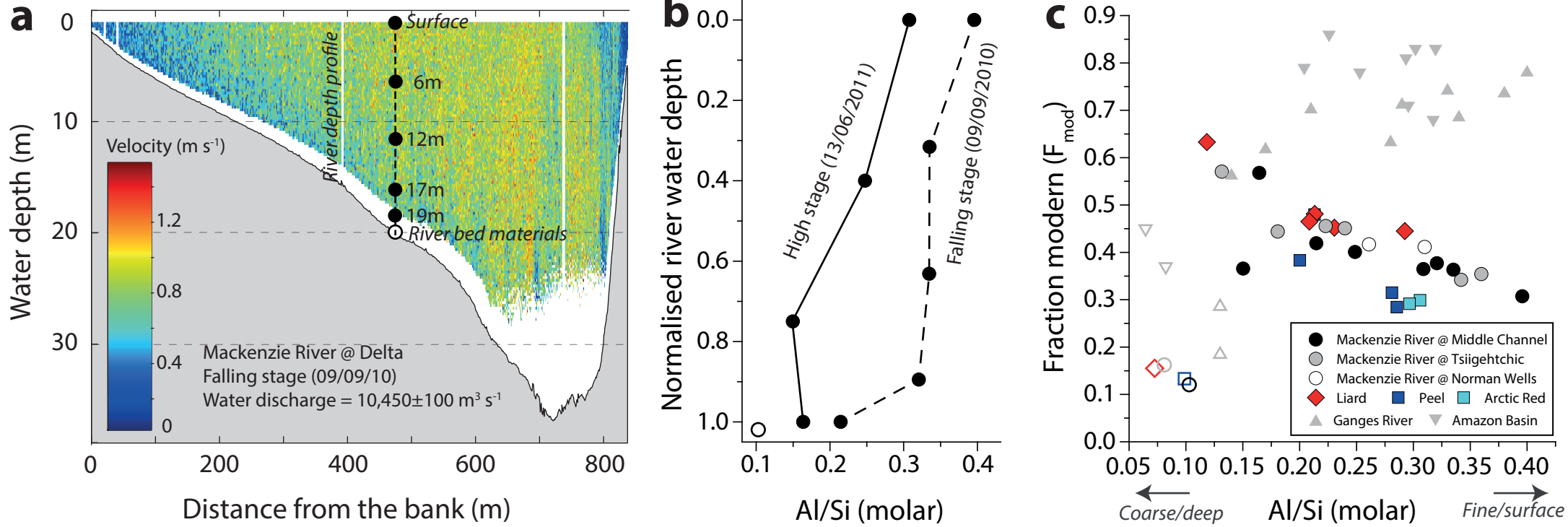


Figure 2

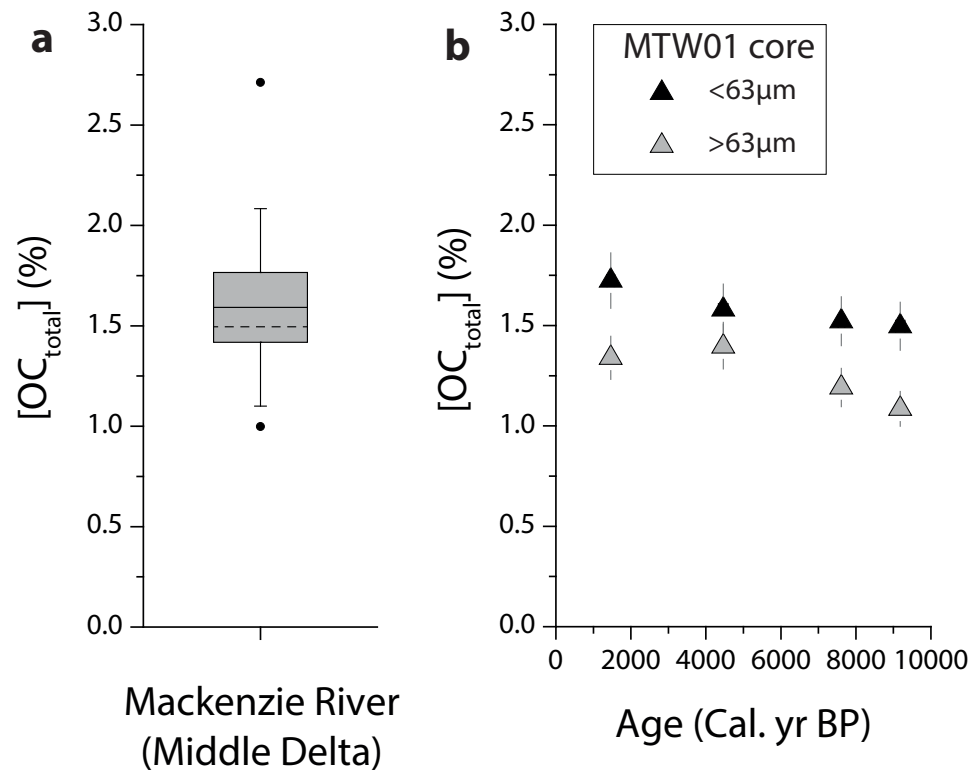


Figure 3